

# A Chandra Grating Observation of the Dusty Wolf-Rayet Star WR 48a

Svetozar A. Zhekov<sup>1</sup>, Marc Gagné<sup>2</sup>, and Stephen L. Skinner<sup>3</sup>

## ABSTRACT

We present results of a *Chandra* High Energy Transmission Grating (HETG) observation of the carbon-rich Wolf-Rayet (WR) star WR 48a. These are the first high-resolution spectra of this object in X-rays. Blue-shifted centroids of the spectral lines of  $\sim -360 \text{ km s}^{-1}$  and line widths of  $1000 - 1500 \text{ km s}^{-1}$  (FWHM) were deduced from the analysis of the line profiles of strong emission lines. The forbidden line of Si XIII is strong and not suppressed, indicating that the rarified 10-30 MK plasma forms far from strong sources of far-UV emission, most likely in a wind collision zone. Global spectral modeling showed that the X-ray spectrum of WR 48a suffered higher absorption in the October 2012 *Chandra* observation compared to a previous January 2008 *XMM-Newton* observation. The emission measure of the hot plasma in WR 48a decreased by a factor  $\sim 3$  over the same period of time. The most likely physical picture that emerges from the analysis of the available X-ray data is that of colliding stellar winds in a wide binary system with an elliptical orbit. We propose that the unseen secondary star in the system is another WR star or perhaps a luminous blue variable.

*Subject headings:* stars: individual (WR 48a) — stars: Wolf-Rayet — X-rays: stars — shock waves

## 1. Introduction

WR 48a is a carbon-rich (WC) Wolf-Rayet star with a WC8 spectral classification (van der Hucht 2001) that was discovered in a near-infrared survey by Danks et al. (1983).

---

<sup>1</sup>Space Research and Technology Institute, Akad. G. Bonchev str., bl.1, Sofia 1113, Bulgaria; szhekov@space.bas.bg

<sup>2</sup>Department of Geology and Astronomy, West Chester University, West Chester, PA 19383, USA; mgagne@wcupa.edu

<sup>3</sup>CASA, University of Colorado, Boulder, CO 80309-0389, USA; stephen.skinner@colorado.edu

This WC star is located inside the G305 star-forming region in the Scutum Crux arm of the Galaxy. Its proximity (within  $2'$ ) to the two compact infrared clusters Danks 1 and 2 suggests that WR 48a likely originates from one or the other (Danks et al. 1984). The optical extinction toward WR 48a is very high,  $A_V = 9.2$  mag (Danks et al. 1983), and only a small part of it is due to circumstellar material (Baume et al. 2009). The distance to WR 48a is not yet well-constrained and various studies provide a range of  $1.21 - 4$  kpc (e.g., van der Hucht 2001; Baume et al. 2009; Danks et al. 1983).

The evolution of its infrared emission suggests that WR 48a is a long-period episodic dust-maker (Williams 1995). This was confirmed by a recent study that revealed recurrent dust formation on a time scale of more than 32 years which also indicates that WR 48a is very likely a wide colliding-wind binary (Williams et al. 2012). However, the interpretation of the nature of WR 48a may not be straightforward. Recently, Hindson et al. (2012) reported the detection of a *thermal* radio source (spectral index  $\alpha = 0.6$ ,  $F_\nu \propto \nu^\alpha$ ) associated with WR 48a, while as a rule wide colliding-wind binaries are *non-thermal* radio sources (Dougherty & Williams 2000).

Nevertheless, the binary nature of WR 48a is further supported by its X-ray characteristics. Analysis of the *XMM-Newton* spectra of WR 48a showed that its X-ray emission is of thermal origin and this is the most X-ray luminous WR star in the Galaxy detected so far, after the black-hole candidate Cyg X-3 (Zhekov, Gagné & Skinner 2011). The latter is valid provided WR 48a is associated with the open clusters Danks 1 and 2 and is thus located at the distance of  $\sim 4$  kpc (Danks et al. 1983).

It is important to recall that all the previous pointed X-ray observations of a small sample of presumed single WC stars have yielded only non-detections, demonstrating that they are X-ray faint or X-ray quiet (Oskinova et al. 2003; Skinner et al. 2006). Therefore, the high X-ray luminosity of the WC star WR 48a is a clear sign that it is not a single star and it is very likely that its enhanced X-ray emission originates from the interaction region of the winds of two massive binary components (Prilutskii & Usov 1976; Cherepashchuk 1976).

In this paper, we report results from the first grating observation of the dusty WR star WR 48a. In Section 2, we briefly review the *Chandra* HETG observation. In Section 3, we present an overview of the X-ray spectra. In Section 4, we analyze the profiles and ratios of strong X-ray emission lines. In Section 5, we present the results from the global spectral fits. We discuss the results from our analysis in Section 6 and list our conclusions in Section 7.

## 2. Observations and Data Reduction

WR 48a was observed with the *Chandra* HETG and ACIS-S detector on 2012 October 12 (*Chandra* ObsId: 13636) with a total effective exposure of 98.6 ksec. Following the Science Threads for Grating Spectroscopy in the CIAO 4.4.1<sup>1</sup> data analysis software, the first-order MEG/HEG and the zeroth-order HETG spectra were extracted<sup>2</sup>. The total source counts were 2083 (MEG), 1456 (HEG) and 4478 (HETG-0), where the MEG and HEG counts are for the +1 and –1 orders combined. The *Chandra* calibration database CALDB v.4.5.0 was used to construct the response matrices and the ancillary response files. For the spectral analysis in this study, we made use of version 11.3.2 of XSPEC (Arnaud 1996).

## 3. An Overview of the X-ray Spectra

As shown in the analysis of the *XMM-Newton* data (Zhekov, Gagné & Skinner 2011), WR 48a is the most X-ray luminous WR star in the Galaxy, after the black hole candidate Cyg X-3, and its spectrum is subject to considerable X-ray absorption. The 5 year time interval between the *XMM-Newton* and *Chandra* observations provides an opportunity to search for any changes of the X-ray emission that may have occurred. From such a comparison, we can immediately conclude that the source has become weaker and its X-ray absorption has increased, as illustrated by the following.

Since the previous *XMM-Newton* observation provided undispersed spectra of WR 48a, it is natural to compare them with the undispersed HETG-0 spectrum from the new *Chandra* observation. We used the two-shock model that perfectly fits the *XMM-Newton* spectra (see Table 1 in Zhekov, Gagné & Skinner 2011) to simulate in XSPEC the expected HETG-0 spectrum by adopting the response matrix and the ancillary file as derived for the *Chandra* observation (see § 2). This procedure yields a predicted HETG-0 spectrum that assumes there were no changes in the X-ray emission of WR 48a between the two observations. Figure 1 shows two versions of the simulated HETG-0 spectrum: one with the nominal values of the two-shock model (absorption, temperature, emission measure) based on the *XMM-Newton* results and one with the emission measure (intrinsic flux) decreased by a factor of 3 (absorption and temperature are kept the same). By comparing the left and right panels in

---

<sup>1</sup>Chandra Interactive Analysis of Observations (CIAO), <http://cxc.harvard.edu/ciao/>

<sup>2</sup>We note that the associated errors for the grating spectra are based on Gehrels (1986). This is the default statistical error for extracting such spectra with CIAO since as a rule the grating spectra have a small number of counts in the individual spectral bins.

Fig 1, we conclude that the absorption was higher during the 2012 *Chandra* observation than during the 2008 XMM-Newton observation. In addition, the rescaled *Chandra* spectrum in Fig.1-right shows that the emission measure during the *Chandra* observation was about a factor of  $\sim 3$  lower than during the *XMM-Newton* observation. In § 5, we will further analyze and discuss this overall change in the X-ray spectrum of WR 48a.

#### 4. Spectral Lines

Due to the decrease in X-ray brightness of WR 48a between the two observations, fewer counts were obtained in the *Chandra* spectra than were anticipated. As a result, we were only able to derive reliable information for a few of the brightest lines in the grating spectra. We re-binned the first-order MEG and HEG spectra every two bins to improve the photon statistics in the individual spectral bins<sup>3</sup>. For the Si XIII, S XV and Fe XXV He-like triplets, we fitted a sum of three Gaussians and a constant continuum. The centers of the triplet components were held fixed according to the AtomDB data base (Atomic Data for Astrophysicists)<sup>4</sup> and all components shared the same line width and line shift. Similarly (with a sum of two Gaussians), we fitted the Si XIV and S XVI H-like doublets but the component intensity ratios were fixed at their atomic data values.

Figures 2, 3 and Table 1 show the results from the fits to the line profiles in the X-ray grating spectra of WR 48a. Only the Si XIII and Si XIV lines are of acceptable quality for determining whether significant line centroid shifts are present (see Fig. 2). These two lines are blue-shifted in the *Chandra* observation of Oct 2012. This is further supported by results for the the S XV line but the data quality in that part of the spectrum is not as good (e.g., near the forbidden line at  $\sim 5.1\text{\AA}$ ). The other two lines which were analyzed show a red-shift (S XVI) or a zero-shift (Fe XXV) but this may well be a result of their poorer photon statistics. Similarly, the Si XIII and Si XIV line results show line broadening of about  $1000 - 1500 \text{ km s}^{-1}$ , while the lines at shorter wavelengths seem to be unresolved in the MEG and HEG spectra (e.g., their line widths are consistent with a zero width, namely, the lower limit of the  $1\sigma$  confidence interval is zero; see Table 1) which is again likely a result of the lower data quality (fewer counts) in these lines.

We checked all the fit results by further improving the photon statistics in individual

---

<sup>3</sup>The bin sizes of the re-binned spectra are  $0.01\text{\AA}$  and  $0.005\text{\AA}$  for the MEG and HEG spectra, respectively. The resolution element (FWHM) is  $0.023\text{\AA}$  (MEG) and  $0.012\text{\AA}$  (HEG): see Table 8.1 in the *Chandra* POG; <http://asc.harvard.edu/proposer/POG/html/index.html>

<sup>4</sup>For AtomDB, see <http://www.atomdb.org/>

spectral bins. Namely, we re-binned the spectra every four bins at the expense of some loss of spectral resolution: the bin size after rebinning was  $0.02\text{\AA}$  (MEG) and  $0.01\text{\AA}$  (HEG). The fits to these heavily re-binned spectra confirmed our basic findings, that is blue-shifted Si XIII, Si XIV and S XV lines. As expected from the coarser binning, the widths of all the lines were consistent with a zero width, namely, the lower limit of the  $1\sigma$  confidence interval was zero.

We also adopted a different approach to the line profile fitting by making use of a statistic different from the standard  $\chi^2$ -statistic. Namely, we made use of the implementation of the Cash statistic (Cash 1979) in XSPEC. The fit results were very similar to those discussed above: the fit parameters were within 5-15% of the values with  $\chi^2$ -statistic and they were tighter constrained (the errors were 45-60% of the values derived if using the standard  $\chi^2$ -statistic; see Table 1).

Finally, to check whether the derived results from the line profile fits are sensitive to the ‘local’ level of continuum, we performed a ‘global-continuum’ fit. Namely, we fitted *simultaneously* all the lines discussed above by introducing a common continuum for all the lines, represented by bremsstrahlung emission with a plasma temperature  $kT = 3\text{ keV}$ . (Fits with a variable plasma temperature were equally successful.) The line profiles were modeled as above, that is by a sum of two or three Gaussians for the doublet and triplet lines, respectively. This ‘global-continuum’ fit provided line parameters that were identical to the ones given in Table 1. These consistency checks provide additional confidence in the derived spectral line parameters despite their relatively large uncertainties.

## 5. Global Spectral Fits

The infrared variability of WR 48a suggests that it is a long-period dust maker, thus, it is likely a long-period WR+O binary system (Williams 1995; Williams et al. 2012). The *XMM-Newton* observation of its X-ray emission provided additional support for its suspected binary nature by discovering that WR 48a is a luminous X-ray source with high plasma temperature (Zhekov, Gagné & Skinner 2011). All these characteristics indicate that colliding stellar winds (CSW) may play an important role in the physics of this object. We recall that as a result of CSWs a two-shock structure forms between the two massive stars in the binary system. This structure is a source of X-ray emission (Prilutskii & Usov 1976; Cherepashchuk 1976) and it is believed to give rise to the variable infrared emission (dust emission; e.g. Williams et al. 1990). We will thus explore the CSW picture in the analysis of the *Chandra* spectra of WR 48a. The best way of doing this is to confront the results from hydrodynamic modeling of CSWs in WR 48a with the observations. However, basic physical

parameters needed to construct a detailed model such as the stellar wind parameters and the binary separation are not available. We will therefore adopt a simplified approach based on discrete-temperature plasma models. We emphasize that discrete-temperature models are a simplified representation of the temperature-stratified CSW region (see Section 5.2 in Zhekov 2007 for discussion of CSW models versus discrete-temperature models). In this as well is in our previous study of the X-ray emission from WR 48a (Zhekov, Gagné & Skinner 2011), we adopted the discrete-temperature model *vpshock* in XSPEC. It is a physical model of the X-ray emission behind a strong plane-parallel shock that takes into account the effects of non-equilibrium ionization (for details of the model see Borkowski et al. 2001).

As demonstrated in § 3, apparent changes have occurred in the X-ray emission of WR 48a between January 2008 October 2012. Namely, the X-ray emission became weaker and more absorbed (Fig. 1). Such changes are possible in the standard CSW picture even for steady-state stellar winds (i.e. mass-loss rates and wind velocities are constant in time). For example, if the orbital inclination is considerably higher than zero degrees then higher X-ray absorption should be detected for orbital phases when the star with the more massive wind in the binary is ‘in front’ (e.g., at azimuthal angles around  $\omega \approx 0^\circ$ ; see Fig. 4). In a WR+O binary this occurs when the WR star is located between the observer and the CSW region. This change (increase) in absorption will occur when the WR star is ‘in front’ regardless of whether the orbit is circular or elliptical. On the other hand, the intrinsic X-ray luminosity of CSWs will change during the orbit only in the case where the orbit is elliptical. We recall that there exists a scaling law for the CSW X-ray luminosity with the mass-loss rate ( $\dot{M}$ ), wind velocity ( $v$ ) and binary separation ( $D$ ):  $L_X \propto \dot{M}^2 v^{-3} D^{-1}$  (Luo et al. 1990; Myasnikov & Zhekov 1993). We thus see that even for constant mass-loss rate and wind velocity the intrinsic CSW luminosity will vary due to the change of the binary separation if the orbit is elliptical.  $L_X$  will reach its maximum near periastron (at the minimum value of  $D$ ) and will have its minimum at apastron (the maximum value of  $D$ ). We will next explore the CSW picture in the analysis of the *Chandra* spectra of WR 48a by assuming that (most of) its X-ray emission originates in CSWs.

We note that all of the global spectral models considered in this study have the following basic characteristics. Since no appreciable excess in the X-ray absorption above that expected from the ISM was found in the analysis of the *XMM-Newton* spectra of WR 48a, the column density of the interstellar X-ray absorption was kept fixed to  $N_{H,ISM} = 2.30 \times 10^{22} \text{ cm}^{-2}$  (see Table 1 in Zhekov, Gagné & Skinner 2011). The additional X-ray absorption that is observed in the *Chandra* spectra (see § 3 and Fig. 1) is attributed to the wind absorption in the more massive WR wind in the presumed WR+O binary. The *vphabs* model in XSPEC was used for this additional absorption component and we enforced its abundances to be the same as that of the emission component(s). The abundances of the emission component(s)

are with respect to the typical WC abundances (van der Hucht et al. 1986) and they were kept fixed to their values derived in Zhekov, Gagné, & Skinner (2011; see the 2T-shock model in Table 1 therein)<sup>5</sup> These values were (expressed as scaling factors to be applied to the typical WC abundances): He = 1, C = 1, N = 1, Ne = 0.11, Mg = 0.13, Si = 0.64, S = 1.78, Ar = 2.78, Ca = 1.97, Fe = 1.31. In our analysis, the total (summed) first-order MEG and HEG spectra and the zeroth-order HETG spectra were fitted simultaneously. To improve the photon statistics, the spectra were re-binned to have a minimum of 20 counts per bin. Based on the results from the line profile analysis (§ 4), a typical line broadening of FWHM = 1000 km s<sup>-1</sup> and a typical line shift of -365 km s<sup>-1</sup> were assumed.

Let us now attribute the entire X-ray emission from WR 48a to the CSWs in a presumed WR+O binary. We recall that if the binary orbit is circular, no changes of the intrinsic X-ray parameters are expected with the orbital phase while the X-ray luminosity may vary if the orbit is elliptical. We denote these two cases  $CSW_{circ}$  and  $CSW_{ell}$ , respectively.

$CSW_{circ}$ . In this case, we made use of the two-shock model that successfully fitted the *XMM-Newton* spectra of WR 48a (see the 2T-shock model in Table 1 in Zhekov, Gagné & Skinner 2011; the model uses the *vpshock* model in XSPEC in conjunction with the XSPEC command *xset neivers* 2.0 to select version 2.0 of the non-equilibrium ionization collisional plasma model). All the model parameters were kept fixed to their values as derived in that analysis. Since excess X-ray absorption is seen in the *Chandra* data (see § 3 and Fig. 1), the two shock components suffer additional *wind* absorption as described above. We first assumed that both emission components have equal wind absorptions. This resulted in a very poor-quality spectral fit (reduced  $\chi^2 \approx 9$ ). If different X-ray absorptions for each component were allowed, the quality of the fit improved but was still statistically unacceptable (reduced  $\chi^2 = 3.2$ ; see Table 2 for details). We can thus conclude that the physical picture of CSW in a WR+O binary that has a *circular* orbit is not supported by the X-ray observations of WR 48a. Namely, such a picture cannot explain the observed changes in the X-ray emission from this object.

$CSW_{ell}$ . In this case, we made use of the same model as above ( $CSW_{circ}$ ) but we also allowed the shock emission measure to vary. This means that we assumed that the shape of the intrinsic X-ray emission does not change with the orbital phase and only the amount

---

<sup>5</sup> Abundances in XSPEC are set by the *abund* command which reads a default file that nominally contains the fractional abundance by number of each element relative to hydrogen (e.g. for solar abundances H = 1.0, He = 0.097, etc.). To simulate nonsolar abundances for He-rich but H-depleted WC stars the default abundance file is modified such that He is assigned a very high abundance relative to H (H = 1.0, He = 50. in our simulations) and the remaining elements are then scaled to their appropriate number fractions relative to He based on the values given in van der Hucht et al. (1986).

of the X-ray emitting plasma does. In other words, although the distance between the stars in the binary varies it does not become very small, so, the stellar winds still have enough space to reach their terminal velocities before they collide. We believe that this is a reasonable assumption for a wide binary system having a long period orbit as is likely the case with WR 48a (its orbital period is at least of 32 years; e.g., Williams et al. 2012). In the fitting procedure, we kept all the shock plasma parameters fixed to their values in the original two-shock model (see the 2T-shock model in Table 1 in Zhekov, Gagné & Skinner 2011). We allowed the total emission measure to vary but we kept the ratio of the emission measures of the shock components fixed to its value as derived in the analysis of the *XMM-Newton* spectra. By fixing this ratio, the shape of the X-ray spectrum is not allowed to vary. Both models with a common (equal) or with a different X-ray absorption for each shock component gave very good fits to the observed *Chandra* HETG spectra. Figure 5 and Table 2 present the results for the case with a separate X-ray absorption for each emission component (i.e. for each shock). The model fit with equal wind absorptions had  $\chi^2/\text{dof} = 251/349$  and it gave identical plasma parameters with the ones presented in Table 2. The common wind absorption was practically a mean of the values given in that table, namely  $N_{\text{He},\text{wind}} = 0.16^{+0.01}_{-0.01} \times 10^{21} \text{ cm}^{-2}$ . The basic result from the CSW<sub>ell</sub> case is that in October 2012 the intrinsic X-ray emission (the amount/emission measure of hot plasma as well) of WR 48a was by a factor  $\sim 3$  lower than its value in January 2008 and the level of the X-ray attenuation increased at the same time, as anticipated in § 3.

In the framework of the standard CSW picture in a binary with an elliptical orbit, the lower X-ray luminosity should be observed when the binary separation is larger. This means that the orbital orientation of WR 48a is such that in October 2012 the binary separation was larger than it was in January 2008. To have an increased value of the X-ray attenuation, the star with the more massive wind should be nearly ‘in front’ in October 2012 (i.e. azimuthal angles around  $\omega \approx 0^\circ$ ; see Fig. 4), so then its counterpart was likely ‘in front’ in January 2008 (i.e. azimuthal angles around  $\omega \approx 180^\circ$ ; see Fig. 4). This seems to be the case since the X-ray absorption (neutral hydrogen column density) showed no appreciable excess above the interstellar value in January 2008 (Zhekov, Gagné & Skinner 2011). However, if the WR star is ‘in front’ the plasma in the interaction region will be outflowing (see Fig. 4), that is it is moving away from the observer. Since the WR wind is expected to be dominant in the system, the CSW ‘cone’ will have its apex pointing towards the WR star (and the observer as well). But instead we found blue-shifted spectral lines in the X-ray spectrum of WR 48a in October 2012 (see § 4) which indicates that the X-ray emitting plasma was moving towards the observer. This suggests that the star with the weaker wind was ‘in front’ at the time of the *Chandra* observation in October 2012 (i.e. azimuthal angles around  $\omega \approx 180^\circ$ ; see Fig. 4). We will return to this apparent discrepancy in § 6.



## 6. Discussion

The most important results from the analysis of the *Chandra* HETG spectra of WR 48a are the following: (i) blue-shifted and broadened (spectrally resolved) emission lines are detected; (ii) in October 2012, the emission measure of the hot gas is about a factor of  $\sim 3$  lower than it was in January 2008; (iii) the X-ray absorption has increased considerably over the same period of time.

As discussed above (§ 5), the CSW picture was adopted in our analysis of the entire X-ray emission from WR 48a. It was done in a simplified manner by making use of a two-shock model. We recall that the CSW region is temperature-stratified and the two-temperature plasma (two-shock model) is just a simplified representation of the temperature stratification of its hot plasma weighted by its emission measure. Thus, we believe that the results derived from the two-shock modeling (the last two mentioned above) are definitely valid in the CSW picture. To double check these two results, we also fitted the HETG spectra with a one-shock model. The results from this model fitting also confirmed the decrease of emission measure by the same factor ( $\sim 3$ ) and the increased (wind) absorption (see 1T-shock model in Table 2). It is worth noting that the success of the single-temperature shock model in this case is due to the fact that the X-ray spectrum of WR 48a is heavily absorbed. However, we have given preference to the two-shock model in our analysis (§ 5) for consistency with the previous study of the X-ray emission of WR 48a in which a two-shock model was required to match the observed spectra successfully (Zhekov, Gagné & Skinner 2011).

As already mentioned, each of the three most important results from this study can be explained in the framework of the CSW picture. Namely, the blue-shifted emission lines indicate that the star with the less powerful wind was globally ‘in front’ of the CSW region at the time of the *Chandra* observation. On the other hand, the decrease of the emission measure over a period of almost 5 years is a sign of an elliptical orbit in the presumed WR+O binary system. Finally, the increased X-ray absorption in October 2012 compared to that in January 2008 indicates that we observed the X-ray emission from the CSW region through a massive stellar wind in the former and likely through the hot gas of the CSW region (or at an orbital phase far from conjunction, thus, no wind absorption) in the latter. But, can we get simultaneously these three observational facts to be consistent with the CSW picture? We believe it is possible in the following, although quite speculative, way.

Suppose the binary system in WR 48a consists of two massive stars: a WR star (of the WC subtype) being the primary in the system and a secondary star which is not an O star but instead a WR or a LBV (luminous blue variable) star. (The latter LBV case might be an object similar to the SMC star HD5980; see Koenigsberger et al. 2010 and references therein.) Suppose the stellar wind of the WC primary is more powerful than that of the secondary.

In the case of an elliptical orbit, the decrease of the emission measure of the CSW region between January 2008 and October 2012 is then explained by the increase of the binary separation over that period of time. If the secondary star was ‘in front’ (e.g., azimuthal angles around  $\omega \approx 180^\circ$ ; see Fig. 4) at the time of the *Chandra* observation (October 2012), then this would explain the detection of blue-shifted lines in the spectrum of WR 48a. On the other hand, if the secondary is a WR or LBV star the high X-ray *wind* absorption is also expected at this orbital phase provided the orbital inclination is high enough. In fact, if the latter is close to 90 degrees and the orbital phase at which the secondary is ‘in front’ has not yet passed, the X-ray absorption will keep increasing. Alternatively, if that orbital phase has already passed the X-ray absorption is already beyond its maximum and it will be decreasing in the future. This would be a secondary maximum for the X-ray absorption since its primary maximum will occur when the primary star (WC) is ‘in front’ (e.g., azimuthal angles around  $\omega \approx 0^\circ$ ; see Fig. 4). And to explain the low (negligible) *wind* absorption in the January 2008 *XMM-Newton* observation, we should assume that at that time we observed the CSW region through its hot gas. This means that the line-of-sight intercepted the CSW ‘cone’ itself (bounded by the two shock surfaces) which eliminates the wind absorption. If this were the case, we may expect that after the phases with increased X-ray absorption have passed (see above) we will witness another phase with low wind absorption which will allow us to directly estimate the opening angle of the CSW ‘cone’. It is worth noting that the chemical composition of the absorbing wind cannot be constrained from the X-ray data alone. We recall that in our analysis the wind absorption component and the emission component share the same abundances. However, successful fits to the HETG spectra were possible even if we assumed that the wind absorption component had a chemical composition typical for interstellar matter. Therefore, our suggestion that the secondary star in the binary might be a WR or a LBV star is not in conflict with the data. Nevertheless, it is worth noting that deep high-resolution optical observations are essential to validate this suggestion.

Finally, we note that the observed changes in the X-ray emission of WR 48a between January 2008 and October 2012 might well be due to some temporary state of the binary system, e.g., they could be a consequence of time-variable stellar wind parameters. Asymmetric stellar winds, having an appreciable contrast of the wind parameters between the stellar pole and equator, could also contribute to those changes. Also, WR 48a could be a system of higher hierarchy than just a wide binary system with a period of  $\geq 32$  years as proposed by Williams et al. (2012). But for interpreting the data in hand, such explanations seem more speculative to us than the one described above. We note that as in the *XMM-Newton* data (Zhekov, Gagné & Skinner 2011) we found no short-term variability in the *Chandra* data of WR 48a. On a timescale less than 100 ksec and time bins between 100 and 2000 s, the X-ray light curve is statistically consistent with a constant flux. On the other hand, even if

the physical picture behind the X-ray emission from WR 48a were more complicated than just CSWs, the latter is likely one of its important ingredients. The strong forbidden line in the He-like triplet of Si XIII (Table 1) is a solid indicator that this line complex forms in a rarefied hot plasma far from strong UV sources which clearly points to a CSW region in a wide massive binary system. It is worth noting that the other He-like triplet detected in the WR 48a spectra, namely S XV, shows enhanced emission from the intercombination line which may indicate a different origin of the very hot plasma where the S XV line complex forms. However, as already mentioned (§ 4) the data in that part of the spectrum are of lower quality and a deeper observation would be needed to validate this result.

## 7. Conclusions

In this work, we presented an analysis of the first grating X-ray spectra of the dusty WR star WR 48a obtained with the *Chandra* HETG. The basic results and conclusions are as follows.

1. From analysis of the line profiles of strong emission lines, a typical line width (FWHM) of  $1000 - 1500 \text{ km s}^{-1}$  was deduced and blue-shifted line centroids of  $\sim -360 \text{ km s}^{-1}$ . A strong (not suppressed) forbidden line in the He-like triplet of Si XIII was detected which indicates that this line forms a rarefied hot plasma far from strong sources of UV emission.
2. Global spectral modeling showed that the X-ray spectrum of WR 48a suffered higher absorption (likely of *wind* origin) in October 2012 (the *Chandra* observation) compared to January 2008 (the *XMM-Newton* observation). The emission measure of the hot plasma in WR 48a decreased by a factor  $\sim 3$  over the same period of time.
3. No X-ray variability on a timescale of less than 100 ksec was detected. This result is similar to what was found from the analysis of the previous X-ray observation of WR 48a with *XMM-Newton* (Zhekov, Gagné & Skinner 2011).
4. The most likely physical picture that emerges from the analysis of the available X-ray data (*Chandra* and *XMM-Newton*) is the following. The high X-ray luminosity of the carbon-rich WR star WR 48a is due to colliding stellar winds in a wide binary system with elliptical orbit. The observed changes of the characteristics (emission measure, absorption) of the X-ray emission of WR 48a and the blue-shift of the line centroids of the strong lines can find their place in the CSW picture, provided the secondary star in the binary system (the companion star of the primary WC object) is not an O star but instead a WR star or a LBV star.

5. More X-ray observations with high spectral resolution are needed to describe in detail the X-ray characteristics of WR 48a. Due to the high X-ray absorption of this object (most of the X-ray emission from WR 48a emerges at energies above 2 keV), *Chandra* HETG data are essential for us to obtain a deeper understanding of the physical picture of CSWs in the fascinating dusty WR star WR 48a.

This work was supported by NASA through *Chandra* Award GO2-13017X to West Chester University, West Chester, Pennsylvania. SAZ acknowledges financial support from Bulgarian National Science Fund grant DO-02-85. The authors thank an anonymous referee for helpful comments and suggestions.

*Facilities:* *Chandra* (HETG).

## REFERENCES

- Arnaud, K.A. 1996, in Jacoby G., Barnes, J. eds., ASP Conf. Ser. Vol. 101, Astronomical Data Analysis Software and Systems, Astron. Soc. Pac., San Francisco, 17
- Baume, G., Carraro, G., & Momany, Y. 2009, MNRAS, 398, 221
- Borkowski, K.J., Lyerly, W.J., & Reynolds, S.P. 2001, ApJ, 548, 820
- Cash, W. 1979, ApJ, 228, 939
- Cherepashchuk, A.M. 1976, Soviet Astronomy Letters, 2, 138
- Danks, A.C., Dennefeld, M., Wamsteker, W., & Shaver, P.A. 1983, A&A, 118, 301
- Danks, A.C., Wamsteker, W., Shaver, P.A. & Retallack, D.S. 1984, A&A, 132, 301
- Dougherty, S.M., & Williams, P.M. 2000, MNRAS, 319, 1005
- Gehrels, N. 1986, ApJ, 303, 336
- Hindson, L., Thompson, M. A., Urquhart, J. S., Faimali, A., Clark, J. S., & Davies, B. 2012, MNRAS, 421, 3418
- Koenigsberger, G., Georgiev, L., Hillier, D. J., Morrell, N., Barba, R., & Gamen, R. 2010, AJ, 139, 2600
- Luo, D., McCray, R., & MacLow, M.-M. 1990, ApJ, 362, 267

- Myasnikov, A.V. & Zhekov, S.A. 1993, MNRAS, 260, 221
- Oskinova, L.M, Ignace, R., Hamann, W.-R., Pollock, A.M.T., & Brown, J.C. 2003, A&A, 402, 755
- Prilutskii, O.F & Usov, V.V. 1976, Soviet Astronomy, 20, 2
- Skinner, S.L., Güdel, M., Schmutz, W. & Zhekov, S.A. 2006, Ap&SS, 304, 97
- van der Hucht, K.A. 2001, New Astronomy Rev., 45, 135
- van der Hucht, K.A., Cassinelli, J.P., & Williams P.M. 1986, A&A, 168, 111
- Williams, P.M. 1995, 'Wolf-Rayet Stars: binaries, colliding winds, evolution', Proceedings IAU Symposium no. 163, eds. K.A. van der Hucht and P.M.Williams, Kluwer Academic Publishers, Dordrecht, 335
- Williams, P.M., van der Hucht, K.A., Pollock, A.M.T., Florkowski, D.R., van der Woerd, H., & Wamsteker, W. 1990, MNRAS, 243, 662
- Williams, P.M., van der Hucht, K.A., van Wyk, F., Marang, F., Whitelock, P.A., Bouchet, B., & Setia Gunawan, D.Y.A.. 2012, MNRAS, 420, 2026
- Zhekov, S.A. 2007, MNRAS, 382, 886
- Zhekov, S.A., Gagné, M. & Skinner, S.L. 2011, ApJ, 727, L17

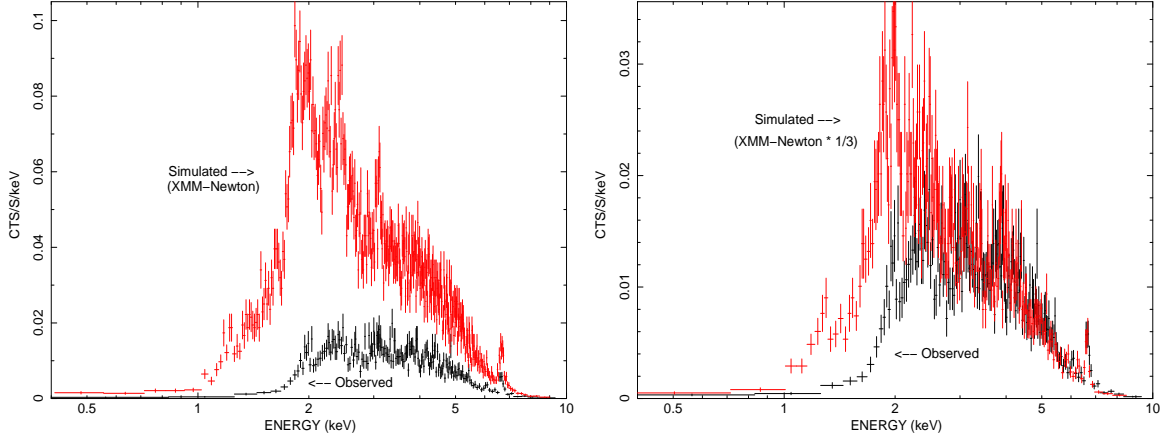


Fig. 1.— The *Chandra* HETG-0 spectrum of WR 48a (black) and the simulated spectrum in XSPEC using the optically-thin plasma model that perfectly fits the *XMM-Newton* EPIC spectra (red). The original spectra are shown in the left panel while in the right panel the simulated spectrum has a reduced flux (emission measure) by a factor of 3.

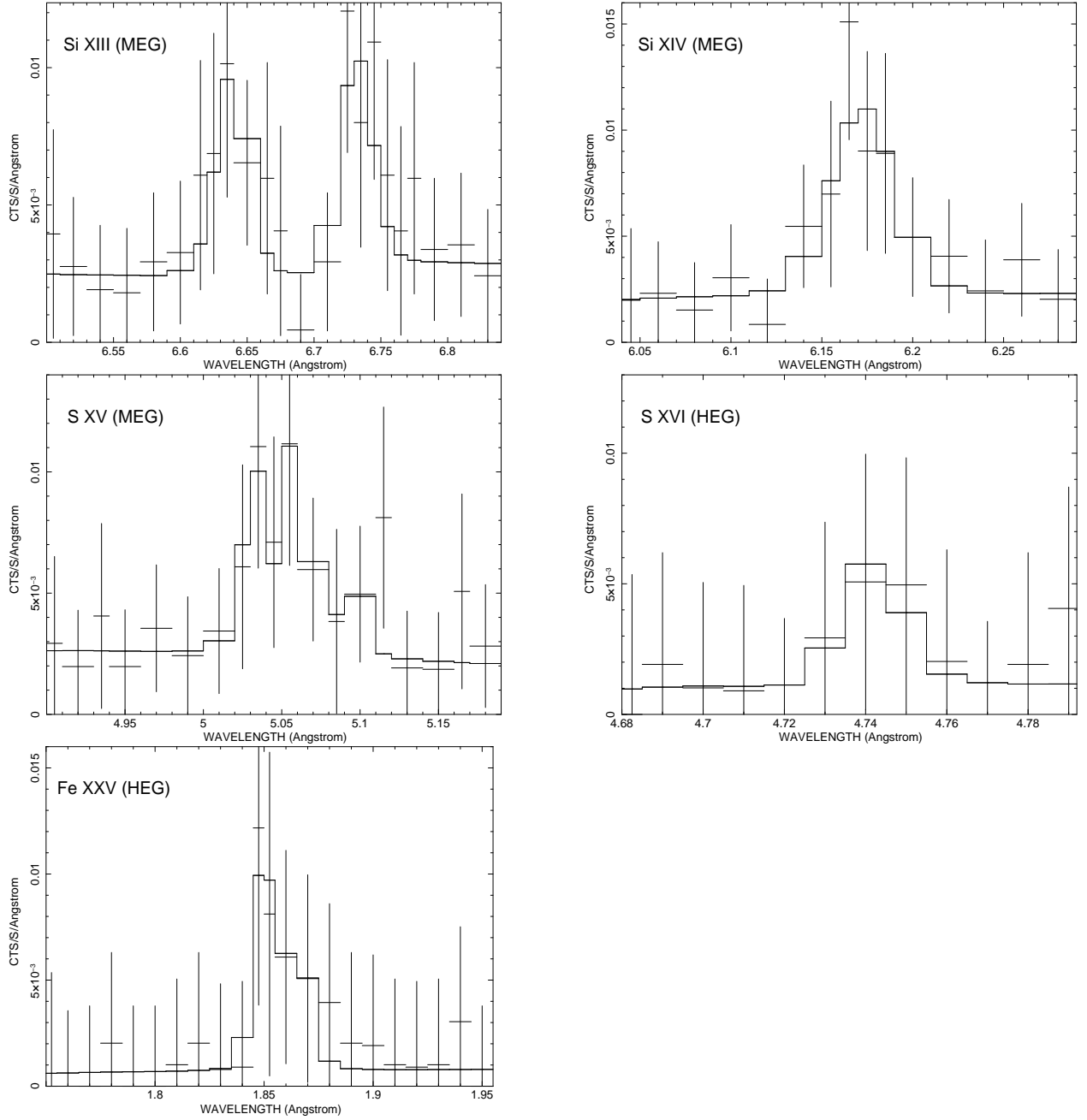


Fig. 2.— Line profile fits to some H-like doublets (Si XIV, S XVI) and He-like triplets (Si XIII, S XV, Fe XXV) in the HEG/MEG first-order spectra of WR 48a. The total number of counts (line+continuum) in all components of a line complex (doublet or triplet) are:  $118 \pm 19$  (Si XIII),  $81 \pm 15$  (Si XIV),  $89 \pm 16$  (S XV),  $16 \pm 11$  (S XVI),  $28 \pm 12$  (Fe XXV). For presentation purposes, the spectra were slightly re-binned with respect to the original binning used in the fits (see § 4).

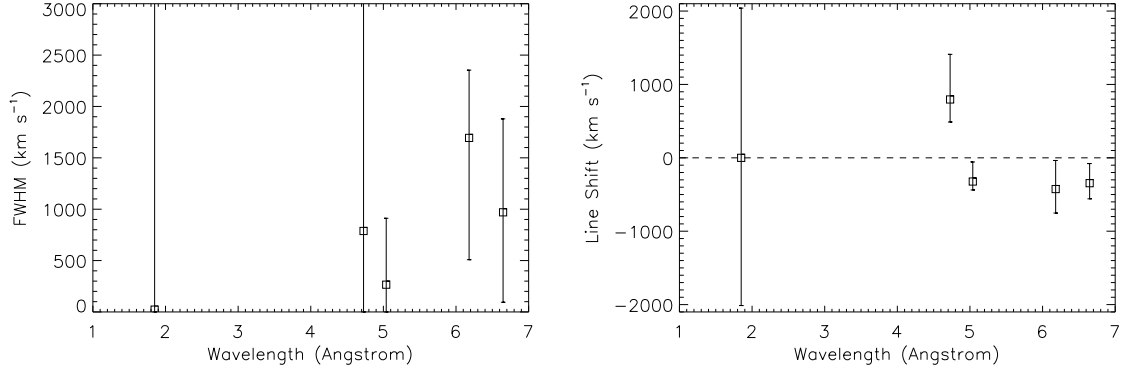


Fig. 3.— Spectral line parameters of WR 48a : Fe XXV (1.85 Å), S XVI (4.73 Å), S XV (5.04 Å), Si XIV (6.18 Å) and Si XIII (6.65 Å). *Left* panel: full width at half maximum (FWHM). *Right* panel: the shift of the centroid of the spectral lines. The error bars correspond to the  $1\sigma$  errors from the line profile fits (see Table 1).



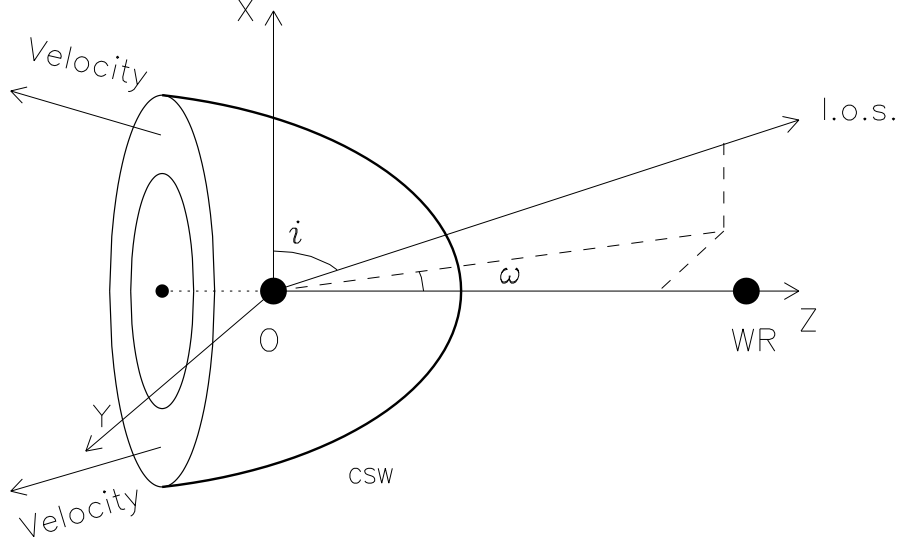


Fig. 4.— A schematic diagram of colliding stellar winds in a massive WR+O binary system. The wind interaction ‘cone’ is denoted by CSW (the axis Z is its axis of symmetry; the axis X is perpendicular to the orbital plane; the axis Y completes the right-handed coordinate system). The line-of-sight towards observer is denoted by l.o.s. and the two related angles,  $i$  (orbital inclination) and  $\omega$  (azimuthal angle) are marked as well. The arrows labeled ‘Velocity’ indicate the general direction of the bulk gas velocity in the interaction region.

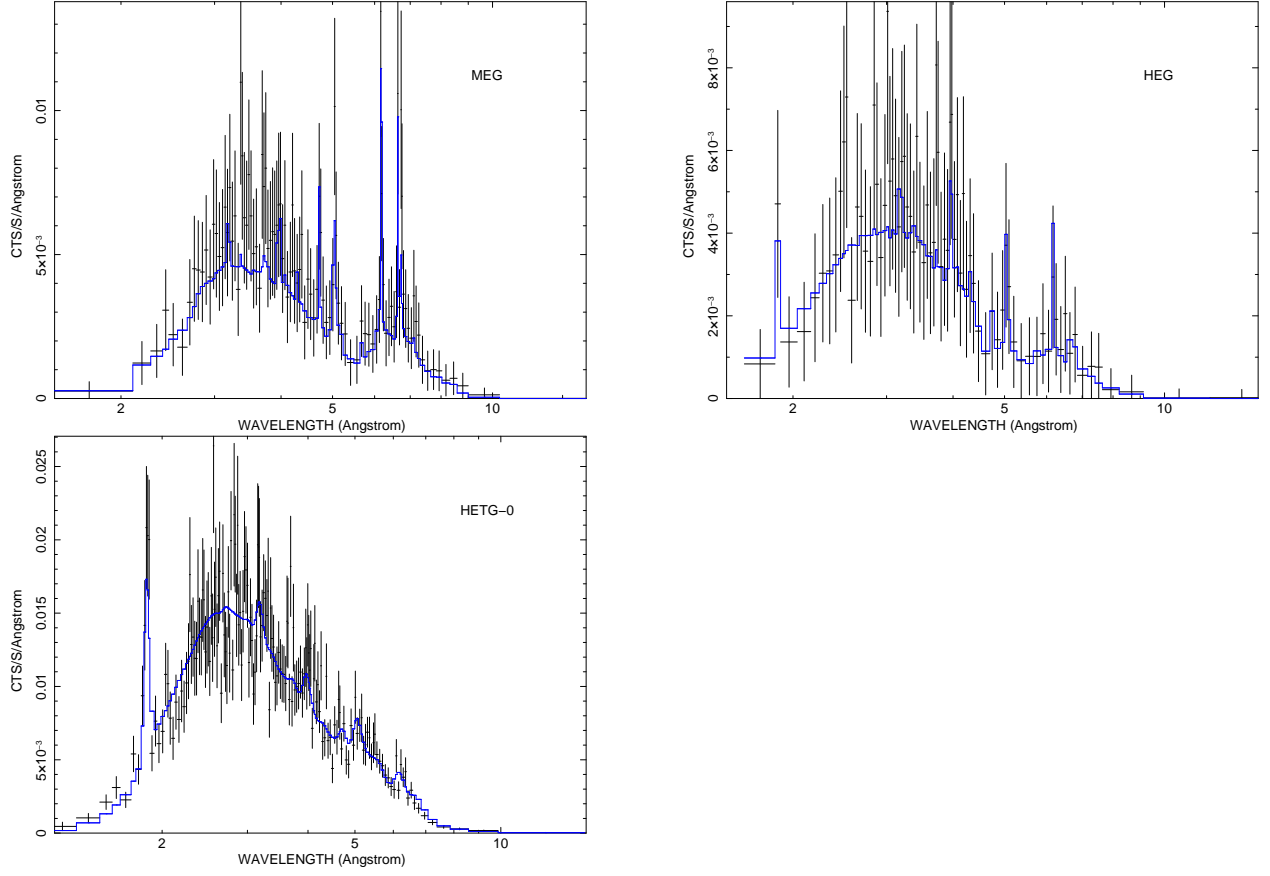


Fig. 5.— The HETG background-subtracted spectra of WR 48a and the two-component model fit (see model  $CSW_{ell}$  in Table 2). The spectra were re-binned to have a minimum of 20 counts per bin.

Table 1. Line Parameters

Line	$\lambda_{lab}^a$ (Å)	FWHM <sup>b</sup> ( km s <sup>-1</sup> )	Line Shift <sup>c</sup> ( km s <sup>-1</sup> )	Flux <sup>d</sup>	Ratio (ATOMDB)
Fe XXV K <sub>α</sub>	1.850	23 <sup>+6001</sup> <sub>-23</sub>	0 <sup>+2040</sup> <sub>-2013</sub>	12.26 <sup>+5.59</sup> <sub>-6.40</sub>	
(i/r) <sup>e</sup>				0.43 <sup>+</sup> <sub>.....</sub>	0.38
(f/r) <sup>e</sup>				0.48 <sup>+</sup> <sub>.....</sub>	0.30
		(1460 <sup>+838</sup> <sub>-864</sub> )	(605 <sup>+309</sup> <sub>-332</sub> )	(12.82 <sup>+3.46</sup> <sub>-2.59</sub> )	
				(0.00 <sup>+0.44</sup> <sub>-0.00</sub> )	0.38
				(0.47 <sup>+0.43</sup> <sub>-0.21</sub> )	0.30
S XVI L <sub>α</sub>	4.727	788 <sup>+2914</sup> <sub>-788</sub>	795 <sup>+614</sup> <sub>-307</sub>	5.32 <sup>+6.12</sup> <sub>-4.79</sub>	
		(794 <sup>+575</sup> <sub>-539</sub> )	(773 <sup>+223</sup> <sub>-215</sub> )	(5.24 <sup>+2.66</sup> <sub>-1.81</sub> )	
S XV K <sub>α</sub>	5.039	265 <sup>+646</sup> <sub>-265</sub>	-323 <sup>+267</sup> <sub>-115</sub>	12.10 <sup>+4.81</sup> <sub>-4.11</sub>	
(i/r)				1.27 <sup>+2.11</sup> <sub>-0.69</sub>	0.23
(f/r)				0.49 <sup>+1.37</sup> <sub>-0.49</sub>	0.44
		(186 <sup>+592</sup> <sub>-186</sub> )	(-356 <sup>+13</sup> <sub>-137</sub> )	(11.83 <sup>+2.89</sup> <sub>-2.41</sub> )	
				(1.63 <sup>+1.46</sup> <sub>-0.61</sub> )	0.23
				(0.74 <sup>+0.76</sup> <sub>-0.34</sub> )	0.44
Si XIV L <sub>α</sub>	6.180	1694 <sup>+659</sup> <sub>-1186</sub>	-426 <sup>+390</sup> <sub>-327</sub>	3.99 <sup>+2.01</sup> <sub>-1.48</sub>	
		(1571 <sup>+963</sup> <sub>-684</sub> )	(-461 <sup>+215</sup> <sub>-222</sub> )	(4.30 <sup>+1.12</sup> <sub>-1.10</sub> )	
Si XIII K <sub>α</sub>	6.648	970 <sup>+909</sup> <sub>-875</sub>	-346 <sup>+268</sup> <sub>-213</sub>	4.71 <sup>+2.07</sup> <sub>-1.76</sub>	
(i/r)				0.00 <sup>+0.22</sup> <sub>-0.00</sub>	0.20
(f/r)				1.03 <sup>+1.01</sup> <sub>-0.52</sub>	0.52
		(869 <sup>+402</sup> <sub>-372</sub> )	(-307 <sup>+105</sup> <sub>-115</sub> )	(5.01 <sup>+1.12</sup> <sub>-0.96</sub> )	
				(0.00 <sup>+0.11</sup> <sub>-0.00</sub> )	0.20
				(1.07 <sup>+0.52</sup> <sub>-0.31</sub> )	0.52

Note. — Results from the fits to the line profiles in the first-order MEG (Si XIII, Si XIV, S XV) and HEG (S XVI, Fe XXV) spectra with the associated  $1\sigma$  errors ( $1\sigma$  error is equivalent to a change in the best-fit statistic value by 1). For the He-like triplets, the flux ratios of the intercombination to the resonance line (i/r) and of the forbidden to the resonance line (f/r) are given as well. The errors on the spectral parameters are those following the Gehrels (1986) recommendation for the cases with a small number of counts in individual data bins (see §2). When we enforced the Gaussian errors on the data (error =  $\sqrt{N}$ ,  $N$  is the number of counts in a data bin), the results from the fits to the line profiles remained within 10-15% of the values given in this Table and the errors from the fits were 40-60% of the values listed here. For comparison in parentheses, given are the results from the fits based on the Cash statistic (Cash 1979).

<sup>a</sup> The laboratory wavelength of the main component.

<sup>b</sup> The line width (FWHM).

<sup>c</sup> The shift of the spectral line centroid.

<sup>d</sup> The observed total multiplet flux in units of  $10^{-6}$  photons  $\text{cm}^{-2} \text{s}^{-1}$ .

<sup>e</sup> Due to the poor photon statistics, these line ratios are not constrained.

Table 2. Global Spectral Model Results

Parameter	CSW <sub><i>circ</i></sub>	CSW <sub><i>ell</i></sub>	1T shock
$\chi^2/\text{dof}$	1107/349	249/348	249/347
$N_{H,ISM}$ ( $10^{22}$ cm $^{-2}$ )	2.30	2.30	2.30
$N_{He,wind,1}$ ( $10^{21}$ cm $^{-2}$ )	$0.12^{+0.01}_{-0.01}$	$0.35^{+0.06}_{-0.14}$	$0.13^{+0.02}_{-0.01}$
$N_{He,wind,2}$ ( $10^{21}$ cm $^{-2}$ )	$2.65^{+0.11}_{-0.07}$	$0.12^{+0.16}_{-0.07}$	
kT <sub>1</sub> (keV)	1.05	1.05	$2.41^{+0.09}_{-0.14}$
kT <sub>2</sub> (keV)	2.82	2.82	
EM <sub>1</sub> ( $10^{54}$ cm $^{-3}$ )	2.42	$0.88^{+0.02}_{-0.02}$	$2.40^{+0.17}_{-0.04}$
EM <sub>2</sub> ( $10^{54}$ cm $^{-3}$ )	5.34	1.94	
$\tau_1$ ( $10^{11}$ cm $^{-3}$ s)	2.42	2.42	$15.9^{+6.70}_{-4.10}$
$\tau_2$ ( $10^{11}$ cm $^{-3}$ s)	8.09	8.09	
$F_X$ ( $10^{-11}$ ergs cm $^{-2}$ s $^{-1}$ )	0.30 (17.7)	0.28 (6.44)	0.27 (2.09)
$F_{X,hot}$ ( $10^{-11}$ ergs cm $^{-2}$ s $^{-1}$ )	0.20 (6.98)	0.26 (2.53)	

Note. — Results from simultaneous fits to the *Chandra* HETG spectra (including both 0-order and 1st-order spectra) of WR 48a (the plasma model used in the fits is the *vpshock* model in XSPEC; see § 5 for details). The abundances were with respect to the typical WC abundances (van der Hucht et al. 1986) and kept fixed to their values derived in Zhekov, Gagné & Skinner (2011). Tabulated quantities are the neutral hydrogen absorption column density ( $N_{H,ISM}$ ), the neutral helium absorption column density (wind absorption;  $N_{He,wind}$ ), plasma temperature (kT), emission measure ( $EM = \int n_e n_{He} dV$ ) for a reference distance of  $d = 1$  kpc ( $EM \propto d^2$ ), shock ionization age ( $\tau = n_e t$ ), the absorbed X-ray flux ( $F_X$ ) in the 0.5 - 10 keV range followed in parentheses by the unabsorbed value ( $F_{X,hot}$  denotes the higher-temperature component). Errors are the  $1\sigma$  values from the fits.